



COVID-19–Associated Nonocclusive Fibrin Microthrombi in the Heart

BACKGROUND: Severe acute respiratory syndrome coronavirus 2 (SARS-CoV-2) and its resultant clinical presentation, coronavirus disease 2019 (COVID-19), is an emergent cause of mortality worldwide. Cardiac complications secondary to this infection are common; however, the underlying mechanisms of such remain unclear. A detailed cardiac evaluation of a series of individuals with COVID-19 undergoing postmortem evaluation is provided, with 4 aims: (1) describe the pathological spectrum of the myocardium; (2) compare with an alternate viral illness; (3) investigate angiotensin-converting enzyme 2 expression; and (4) provide the first description of the cardiac findings in patients with cleared infection.

METHODS: Study cases were identified from institutional files and included COVID-19 (n=15: 12 active, 3 cleared), influenza A/B (n=6), and nonvirally mediated deaths (n=6). Salient information was abstracted from the medical record. Light microscopic findings were recorded. An angiotensin-converting enzyme 2 immunohistochemical H-score was compared across cases. Viral detection encompassed SARS-CoV-2 immunohistochemistry, ultrastructural examination, and droplet digital polymerase chain reaction.

RESULTS: Male sex was more common in the COVID-19 group ($P=0.05$). Nonocclusive fibrin microthrombi (without ischemic injury) were identified in 16 cases (12 COVID-19, 2 influenza, and 2 controls) and were more common in the active COVID-19 cohort ($P=0.006$). Four active COVID-19 cases showed focal myocarditis, whereas 1 case of cleared COVID-19 showed extensive disease. Arteriolar angiotensin-converting enzyme 2 endothelial expression was lower in COVID-19 cases than in controls ($P=0.004$). Angiotensin-converting enzyme 2 myocardial expression did not differ by disease category, sex, age, or number of patient comorbidities ($P=0.69$, $P=1.00$, $P=0.46$, $P=0.65$, respectively). SARS-CoV-2 immunohistochemistry showed nonspecific staining, whereas ultrastructural examination and droplet digital polymerase chain reaction were negative for viral presence. Four patients (26.7%) with COVID-19 had underlying cardiac amyloidosis. Cases with cleared infection had variable presentations.

CONCLUSIONS: This detailed histopathologic, immunohistochemical, ultrastructural, and molecular cardiac series showed no definitive evidence of direct myocardial infection. COVID-19 cases frequently have cardiac fibrin microthrombi, without universal acute ischemic injury. Moreover, myocarditis is present in 33.3% of patients with active and cleared COVID-19 but is usually limited in extent. Histological features of resolved infection are variable. Cardiac amyloidosis may be an additional risk factor for severe disease.

Melanie C. Bois, MD
Nicholas A. Boire, MD, MS
Andrew J. Layman, MD
Marie-Christine Aubry, MD
Mariam P. Alexander, MD
Anja C. Roden, MD
Catherine E. Hagen, MD
Reade A. Quinton, MD
Christopher Larsen, MD
Young Erben, MD
Ramanath Majumdar, PhD
Sarah M. Jenkins, MS
Benjamin R. Kipp, PhD
Peter T. Lin, MD
Joseph J. Maleszewski^{1b}, MD

Key Words: autopsy ■ COVID-19
■ heart ■ pathology ■ SARS-CoV-2

Sources of Funding, see page 242

© 2020 American Heart Association, Inc.

<https://www.ahajournals.org/journal/circ>

Clinical Perspective

What Is New?

- Microthrombosis of the small myocardial vasculature appears to be a relatively common finding in coronavirus disease 2019 (COVID-19) and may persist even after viral clearance, although its significance is not yet established.
- Myocarditis, when present, is usually very limited in extent.
- Direct myocardial injury by the virus does not appear to be a common mechanism of severe acute respiratory syndrome coronavirus 2.

What Are the Clinical Implications?

- The findings suggest a potential role for anticoagulation in patients with COVID-19.
- Patients with preexisting cardiac disease (specifically, cardiac amyloidosis) who develop COVID-19 may be at higher risk for complications (including death).

Coronavirus disease 2019 (COVID-19), the disease caused by severe acute respiratory syndrome coronavirus 2 (SARS-CoV-2), has rapidly emerged as a major global health crisis. Although its primary pathogenic mechanism involves infection of the respiratory tract—mediated through the angiotensin-converting enzyme 2 (ACE2) host cell receptor—other organ systems are not spared. More specifically, cardiovascular complications have increasingly been recognized clinically. Cardiac injury appears to be a source of significant morbidity and mortality in patients with COVID-19, in particular, among those who have preexisting cardiovascular disease. A subset of these diseases is associated with increased ACE2 expression in the heart.^{1,2}

Cardiac injury, variably defined by serological, electrocardiographic, or imaging studies, has been reported in upward of one-third of patients hospitalized with COVID-19 infection.^{3–5} The mechanisms are believed to be multifactorial, including direct effects such as myocarditis, and indirect forms of injury such as thrombosis or demand ischemia imparted by the underlying respiratory issues, as well. The frequency and extent of these different mechanisms has yet to be established.

It is fortunate that pathology-based studies that offer important windows into pathogenic mechanisms have also begun to emerge. These have largely been autopsy based and (again) focused primarily on the pulmonary complications.^{6–10} Several series have reported thrombosis involving the pulmonary and cardiac microvasculature,^{8,10–12} although the extent of this finding and its specificity have not been formally evaluated. In those studies that have reported on cardiovascular

findings, most have described myocardial inflammation that, when present, is typically mild and without myocyte injury.

Herein, we present a series of patients with COVID-19 who underwent postmortem examination, with emphasis on cardiovascular findings. In so doing, we focused on 4 aims: (1) describe the pathological spectrum of the myocardium in patients who have COVID-19 including direct analysis for myocardial virus localization through molecular and ultrastructural means; (2) compare the histopathologic findings with other viral illness, evaluating for findings specific to COVID-19; (3) investigate whether ACE2 expression within the myocardium can correlate with histopathology; and (4) provide the first description of the cardiac findings in patients with cleared infection.

METHODS

The study was deemed exempt from review by the Mayo Clinic Institutional Review Board in accordance with the Code of Federal Regulations, 45 CFR 46.102. Biospecimen use was approved by the Mayo Clinic Institutional Review Board's Biospecimens Sub-Committee (20-004318).

The data that support the findings of this study are available from the corresponding author on reasonable request.

Cohort Selection

All cases of COVID-19, as confirmed by antemortem SARS-CoV-2 nasopharyngeal or oropharyngeal polymerase chain reaction (PCR), undergoing postmortem examination at the Mayo Clinic (Rochester, MN) between April 2 and September 9, 2020, were included. The COVID-19 cohort comprised individuals who were autopsied and who had had a positive antemortem SARS-CoV-2 Immunoglobulin G antibody test through the EUROIMMUN (EUROIMMUN Medizinische Labordiagnostika AG) Anti-SARS-CoV-2 ELISA (Immunoglobulin G) assay. Cases of COVID-19 were considered cleared if the patient demonstrated negative PCR testing either before death or at the time of autopsy, having previously demonstrated either a positive PCR test or positive antibody test.

Two autopsy-derived control cohorts were selected for comparative purposes, including individuals who died of complications associated with influenza A/B infection (sequential; as identified by antemortem or postmortem PCR) and a cohort of individuals who died of nonvirally mediated mechanisms. Postmortem interval (time between death and autopsy/fixation) was documented. Salient information for all cases was abstracted from the medical record, including demographic information, disease history (if available), and the presence or absence of the following chronic underlying conditions, as well: systemic hypertension, hyperlipidemia, type 2 diabetes, chronic kidney disease, and chronic cardiovascular conditions (eg, cardiac amyloidosis, coronary artery disease).

Gross and Histological Examination

All specimens were systematically evaluated grossly by 2 cardiovascular pathologists (M.C.B. and J.J.M.). Hearts were

processed in accordance with specific guidelines for COVID-19 that were internally established at the outset of the pandemic. Hearts were fixed in 10% neutral buffered formalin for a minimum of 24 hours before dissection. Dissection included serial sections from the apex to the base; with dissection of the cardiac base proceeding in an inflow-outflow method. Sampling of a minimum of 5 transmural myocardial sections was performed from the base, midventricular, and apical thirds (including left and right ventricular free walls and septum). If gross abnormalities were noted, sections of such were explicitly included in this collection. Otherwise, samples were procured to represent anterior, lateral, and posterior/inferior regions.

Histopathologic analysis included specific attention to the presence or absence of the following features: thrombosis, myocarditis, interstitial edema, and ischemic changes. The frequency of microvascular thrombi was enumerated through manual and blinded histological review of a transmural section of the left ventricle, documented as a ratio of involved small arteries and arterioles (hereinafter collectively referred to as arterioles) to the total present in the evaluated cardiac section. Microthrombi were counted in left ventricular sections away from acute ischemic injury, where applicable. Chronic underlying findings and cardiac-based comorbidities were documented.

Ultrastructural Examination

Transmission electron microscopy was performed on the COVID-19 study cohort to evaluate for virus. A total of six 1-mm cubes were procured from the basal, midventricular, and apical myocardium, in each case, at the time of autopsy and was fixed in Trump fixative (1% glutaraldehyde and 4% formaldehyde in 0.1 mol/L phosphate buffer, at pH 7.2). Tissue was then rinsed for 30 minutes in 3 changes of 0.1 mol/L phosphate buffer, at pH 7.2, followed by a 50-minute postfix in 1% OsO₄. The tissue was rinsed in 3 changes of distilled water, dehydrated in progressive concentrations of ethanol and 100% acetone, and embedded in epoxy resin. Thin (90-nm) sections were cut, placed on 200 mesh copper grids, and stained with lead citrate. Images were taken on a JEOL 1400 plus electron microscope operating at 80 kV. Cardiac myocytes, endothelial cells, and interstitial fibroblasts were all targeted for this evaluation by a cardiovascular pathologist with special training in electron microscopy (J.J.M.).

Immunohistochemistry: ACE2 Receptor

The tissue sections were stained using a Leica Bond RX stainer (Leica) at the Pathology Research Core (Mayo Clinic). Antigen retrieval used for ACE2 was Epitope Retrieval 2 (EDTA based, Leica) at 100°C for 20 minutes. Some of the reagents from the Polymer Refine Detection System (Leica) were used during the staining process. Tissue sections were incubated in Peroxidase Block (Leica) for 5 minutes and then in Protein Block (Dako) for 5 minutes. The primary antibody for ACE2 (R&D Systems, goat, AF933) was diluted at 1:150 (from a 0.5 µg/µL concentration) in Background Reducing Diluent (Dako) and incubated for 15 minutes. Sections were incubated in secondary antibody and tertiary reagent from the Goat HRP Kit (Biocare Medical LLC) for 15 minutes each. Immunostaining

visualization was achieved by incubating sections in diaminobenzidine (Leica) for 10 minutes and counterstained in hematoxylin for 5 minutes. Once stain was completed, slides were dehydrated in increasing concentrations of ethyl alcohol and cleared in xylene before permanent coverslipping.

Slides were scored separately and in a blinded fashion by 2 cardiovascular pathologists (J.J.M. and M.C.B.) for membranous stain intensity (0=none, 1=dot-like, 2=uniform) and distribution across cells (0=0%, 1=1%–5%, 2=6%–25%, 3=26%–75%, 4≥75%) within the following categories: all endothelium, arteriolar endothelium, and myocardium. An H-score was calculated by the product of the aforementioned parameters, and the agreement between pathologists was calculated.

Immunohistochemistry: SARS-CoV-2

Immunohistochemical assays were performed on the Leica BOND-III platform (Leica) using formalin-fixed, paraffin-embedded specimens sectioned at 3 µm onto positively charged glass slides. Immunohistochemical antigen retrieval was performed using BOND Epitope Retrieval Solution 2 (prediluted, pH 9.0; AR 9640) for 20 minutes at 100°C. Specimens were incubated with mouse monoclonal SARS-CoV-2 nucleocapsid antibody (Bioss) for 15 minutes at room temperature, followed by visualization with the Leica Bond detection kit at room temperature (DS 9800). The specimens were then counterstained with hematoxylin. Immunohistochemical stains were all performed with appropriate positive and negative controls.

Droplet Digital Polymerase Chain Reaction

Droplet digital polymerase chain reaction (ddPCR) was performed on the cardiac tissue from all patients with COVID-19, with paired lung specimens in 9 cases (the latter selected chronologically). Formalin-fixed, paraffin-embedded cardiac and pulmonary specimens underwent nucleic acid extraction by using the Qiagen RNeasy DSP formalin-fixed, paraffin-embedded Kit (Qiagen). ddPCR (Bio-Rad) was performed on extracted nucleic acid to detect SARS-CoV-2 N1 and N2 (nucleocapsid 1 and 2) sequences. Positive cases were defined as those with >4 droplets in either the N1 or N2 target.

Statistical Analysis

Data were summarized with medians and interquartile ranges (IQRs) or ranges, or with frequencies and percentages, as appropriate. Ordinal and continuous data were compared between groups (COVID versus influenza versus control) with Kruskal-Wallis tests; categorical data were compared with Fisher exact tests. Pairwise comparisons were performed (reference=COVID) when the overall test was significant.

The H-score (J.J.M. and M.C.B., including arteriolar, myocardial, and endocardial ACE2 staining) distributions were compared by sex, age (dichotomized at the median: ≤78 versus >78), and total comorbidities (<2 versus ≥2) with Kruskal-Wallis tests. The degree of agreement in H-scores was summarized with the average difference in scores between reviewers, along with the percentage of agreement to within 1 point.

P values ≤ 0.05 were considered statistically significant. All analyses were performed using SAS version 9.4 (SAS Institute Inc) or R (R Core Team [2019], R Foundation for Statistical Computing).

RESULTS

Cohort Characteristics

The study cohort consisted of 15 cases of COVID-19 (12 active; 3 cleared). The study cohort was compared with cohorts in which deaths were attributed to virally mediated (influenza) and nonvirally mediated phenomena, including 6 cases of influenza (influenza A, $n=5$; influenza B, $n=1$) and 6 nonviral infection–associated deaths. Cleared COVID-19 cases included: (1) a decedent with a positive antemortem SARS-CoV-2 PCR, followed by 2 negative swabs before death, with negative PCR at the time of autopsy (postmortem evaluation was performed >2 months after the original positive PCR; the patient was symptomatic from pulmonary complications of COVID-19 at the time of death), and (2) a decedent who had a positive antemortem SARS-CoV-2 immunoglobulin G antibody test with simultaneously negative SARS-CoV-2 PCR, but was otherwise asymptomatic and died of acute heart failure in the setting of ischemic heart disease; and (3) a decedent with a positive SARS-CoV-2 PCR 54 days before death, followed by negative antemortem and postmortem PCR testing, who was placed on extracorporeal membrane oxygenation and subsequently developed *Klebsiella* sp. pneumonia and a bleeding diathesis. Age, sex, and frequency of comorbidities by category are summarized in Table 1 and Table I in the Data Supplement, along with additional clinical and serological parameters. Age and number of comorbidities did not vary significantly among categories ($P=0.2$ and $P=0.18$, respectively). Male sex was more common in the COVID-19 group ($P=0.05$). The mean postmortem interval was 24.5 hours (range: 4 hours 15 minutes to 51 hours 30 minutes). A comparison of active versus cleared COVID-19 cases is provided in Table 2.

The COVID-19 cohort in the study was also compared with the overall hospitalized patient with COVID-19 population at the same institution. In the same period, 153 individuals (52% men) were hospitalized with COVID-19, with a mean age of 56.8 years. In comparison with our postmortem cohort, this suggests that mortality was observed more often in older men, in keeping with observations documented in previous and current literature.

Histological Characteristics

Nonocclusive fibrin microthrombi were identified in 16 cases, of which 12 were COVID-19 (including 1 cleared), 2 influenza, and 2 controls (Figure 1). The

fibrinous nature was confirmed by staining with factor VIII immunohistochemistry, Masson trichrome stain, and phosphotungstic acid hematoxylin (Figure 2). COVID-19 cases showed a mean involvement of 7.4% of arterioles (IQR, 3.1; 8.2%) overall, whereas active COVID-19 cases had a mean involvement of 8.7% (IQR, 5.1; 10.4%). In comparison, influenza and control cases showed mean involvement of 2.0% and 1.0%, respectively (influenza IQR, 0, 5.9%; control IQR, 0; 6.8%; $P=0.003$; Table 3; Figure 3). Many involved arterioles showed endothelial cell lining above the fibrin deposit, whereas others showed acute fibrin thrombi without endothelialization. Acute ischemic changes were observed in 2 COVID-19 cases, 1 of which was devoid of fibrin thrombi in the vasculature. A single case demonstrating fibrin thrombi showed ischemic injury visible by light microscopy.

Two control cases showed fibrin microthrombi, including (1) an individual who died of metastatic pancreatic adenocarcinoma to the peritoneal lymph nodes and lungs, with concomitant acute bronchopneumonia and organizing pneumonia; and (2) a woman with a pulmonary thromboembolism and *Staphylococcus aureus* bronchopneumonia with abscess formation. One influenza case showed microthrombi associated with a large, segmental acute myocardial infarction. The other influenza case demonstrating microthrombi showed acute bronchopneumonia with superimposed *Klebsiella pneumoniae* infection.

Three cases of COVID-19 were without microthrombi. One was a patient with active disease, and the youngest of the cohort (age 29 years). The other 2 cases were cleared infections, 1 case with SARS-CoV-2 immunoglobulin G antibodies, without active disease; and the other case with a history of extracorporeal membrane oxygenation and bleeding diathesis.

Two COVID-19 cases showed mural thrombi; 1 within the right atrium in a patient with a history of paroxysmal atrial fibrillation, and 1 within the apical left ventricle. The patient with a left ventricular mural thrombus had no pertinent imaging providing cardiac function status during his illness. No mural thrombi were identified in the remaining COVID-19, influenza, or control patients.

Active lymphocytic myocarditis was present in 5 patients with COVID-19 (33.3%, 4 with active disease and 1 with cleared infection; Figure 4). The case with a cleared infection showed extensive myocardial involvement with fibrosis and focal active myocyte injury (smoldering myocarditis), whereas the remaining cases showed only focal active myocarditis. One of these cases showed myocarditis associated with amyloid deposition. Active lymphocytic myocarditis was additionally identified in 1 influenza B case. Four (26.7%) of the COVID-19 patients harbored underlying ATTR (transthyretin)-type cardiac amyloidosis.

Table 1. Cohort Demographics and Relevant Clinical Characteristics

Demographics and clinical characteristics	COVID-19* (n=15)	Influenza (n=6)	Controls (n=6)	P value
Age, median (interquartile range)	78 (71–86)	52 (46–80)	74 (65–81)	0.20†
Male sex, n (%)	12 (80.0)	2 (33.3)	2 (33.3)	0.05‡
Comorbidities per patient,§ median (interquartile range)	2 (1–3)	2.5 (1–3)	0.5 (0–1)	0.18†
Medications influencing coagulation, n (%)¶				
Aspirin	5/9 (55.6)	2/3 (66.7)	2/4 (50.0)	1.0‡
Heparin/enoxaparin	2/9 (22.2)	0/3 (0.0)	0/4 (0.0)	1.0‡
Clopidogrel	0/9 (0.0)	0/3 (0.0)	1/4 (25.0)	0.44‡
Apixaban	1/9 (11.1)	0/3 (0.0)	1/4 (25.0)	1.0‡
Warfarin	1/9 (11.1)	0/3 (0.0)	0/4 (0.0)	1.0‡
Coagulation parameters				
Platelet count (×10 ⁹ /L)				
n	12	4	5	0.82†
Median (range)	215 (33–670)	144.5 (55–461)	222 (102–374)	
D-Dimer, ng/mL				
n	7	1	3	0.8†
Median (range)	1145 (1.9–2475)	14065	336 (0–775)	
Prothrombin time, s				
n	9	4	6	0.70†
Median (range)	15.9 (12.2–51.7)	18.7 (12.9–27.6)	15.5 (10.6–91.8)	
Activated partial thromboplastin time				
n	7	4	5	0.22†
Median (range)	32 (27–83)	38.5 (35–63)	35 (24–39)	
International normalized ratio				
n	10	5	6	0.59†
Median (range)	1.5 (1.1–4.6)	1.8 (1.2–2.5)	1.3 (1.0–8.2)	
Thrombin time, s				
n	1	1	1	Not applicable
Median	34.7	28.4	21.6	
Fibrinogen, mg/dL				
n	5	4	2	0.36†
Median (range)	574 (236–774)	465 (345–576)	249 (71–427)	
High-sensitivity troponin, ng/L				
n	8	4	6	0.28†
Median (range)	19.5 (0–461)	82 (28–223)	19 (0–90)	
History of angiotensin-converting enzyme inhibitor use, n (%)	6/9 (66.7)	2/3 (66.7)	0/4 (0)	0.10‡

*Including both patients with active and cleared severe acute respiratory syndrome coronavirus 2 viral infection.

†Kruskal-Wallis test.

‡Fisher exact test.

§Defined as underlying chronic conditions, including systemic hypertension, hyperlipidemia, type 2 diabetes, and chronic kidney disease.

¶Medications immediately preceding or during terminal illness and hospitalization; denominator denoted number of patients in each category with information present in the medical record.

Acute ischemic injury was present in 4 cases (2 COVID-19 cases and 2 influenza cases). Both cases of COVID-19 with acute ischemic injury showed subendocardial foci <0.1 cm in the greatest dimension (1 case

contained a single such focus, and the other showed multifocal findings), histologically ≈12 to 24 hours old. The case with only 1 focus of ischemia did not show histological features of fibrin microthrombi and

Table 2. COVID-19 Cases

Characteristics	Active infection (n=12)	Cleared infection (n=3)
Age, median (interquartile range)	78 (71–86)	78 (51–94)
Male sex, n (%)	12 (80)	2 (67)
Symptomatic at death, n (%)	12 (100)	2 (67)

COVID-19 indicates coronavirus disease 2019.

was a case of active infection. This decedent was the youngest in our cohort (29-years-old) and did not have underlying comorbidities nor did he have significant coronary artery atherosclerosis. Additional histological findings included focal active myocarditis in the right ventricle, acute lung injury (organizing pneumonia and diffuse alveolar damage), and pulmonary thromboemboli. The case with multiple subendocardial ischemic foci showed fibrin microthrombi in 4.8% of arterioles and did have coronary artery disease (grade 3 [of 4]) of the epicardial artery supplying the regional myocardium. This was an active infection in an 84-year-old man with systemic hypertension and hyperlipidemia, who had pulmonary manifestations of diffuse alveolar damage and acute bronchopneumonia.

A summary of the histological findings in patients with COVID-19 is provided in Figure 5, Table 3, and Table II in the Data Supplement.

Ultrastructural Characteristics (Patients With COVID-19)

No virus was identified within the cardiac myocytes, vascular endothelium, or interstitial fibroblasts of

the myocardium in any of the COVID-19 cases reviewed (Figure 6).

ACE2 Receptor Immunohistochemistry

Small artery and arteriolar endothelial expression was reduced in the COVID-19 cohort (mean H-score: J.J.M., 0.93; M.C.B., 1.07) versus noninfluenza controls (mean H-score: J.J.M., 4.17; M.C.B., 4.17; *P* value: J.J.M., 0.004; M.C.B., 0.001). Expression in the COVID-19 group was also reduced in comparison with influenza cases (mean H-score: J.J.M., 1.83; M.C.B., 1.33); however, this parameter was not significant (*P* value: J.J.M., 0.06; M.C.B., 0.57). The average difference between pathologists was low, with a mean of 0.04 (SD, 1.74; *P*=0.91), and with 74% of observations in agreement within 1 point. Five active COVID-19 cases showed no arteriolar staining, as agreed on independently by both pathologists.

Myocardial staining was present in all cases. No statistically significant difference was found by disease category, sex, age, or number of comorbidities (*P*=0.69, *P*=1.00, *P*=0.46, and *P*=0.65, respectively). The average difference of myocardial scoring between pathologists was 0.11 (SD, 1.12; *P* value=0.61), with 70% of observations in agreement within 1 point.

Endothelial staining was not significantly different among categories (*P* values: J.J.M., *P*=0.25; M.C.B., *P*=0.56), with a mean difference between pathologists of −0.26 (SD, 2.3; *P*=0.56). This variable showed the greatest degree of variability between reviewers.

We observed that myocardial staining was typically more intense around small intramural blood vessels.

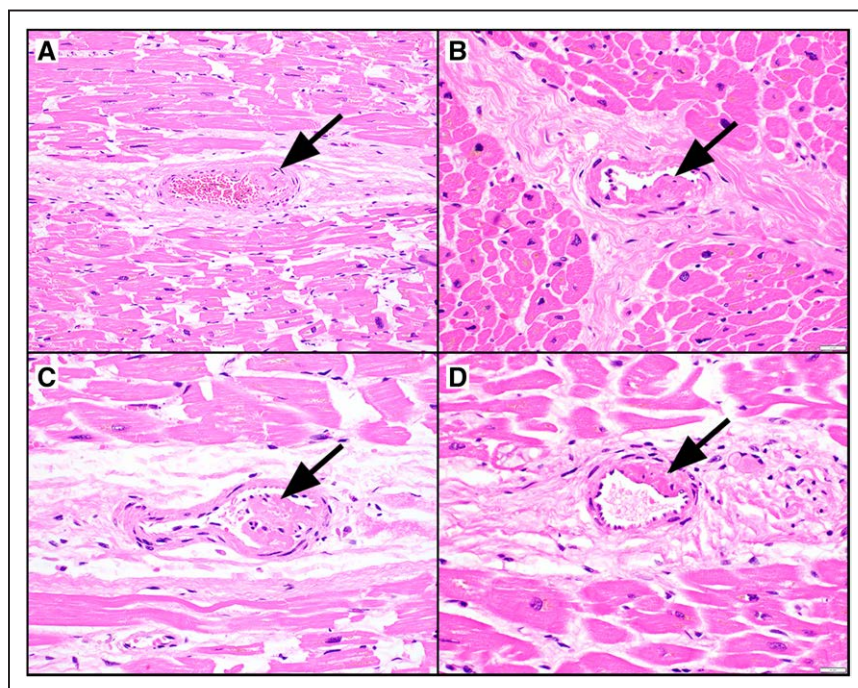


Figure 1. Nonocclusive fibrin microthrombi.

Small arteries and arterioles demonstrated nonocclusive, eccentric fibrin microthrombi without associated histologically identified ischemic injury in the majority of patients with coronavirus disease 2019 (COVID-19). **A** shows a nonocclusive fibrin thrombus (arrow) in an 80-year-old man with active COVID-19. Likewise, these findings were observed in a 78-year-old man who died of severe acute respiratory syndrome coronavirus 2 infection (**B**, arrow). Nonocclusive thrombi were observed projecting into the vessel lumen (**C**, arrow), and with a more eccentric, diminutive intraluminal profile (**D**, arrow) (hematoxylin and eosin, 600× original magnification).

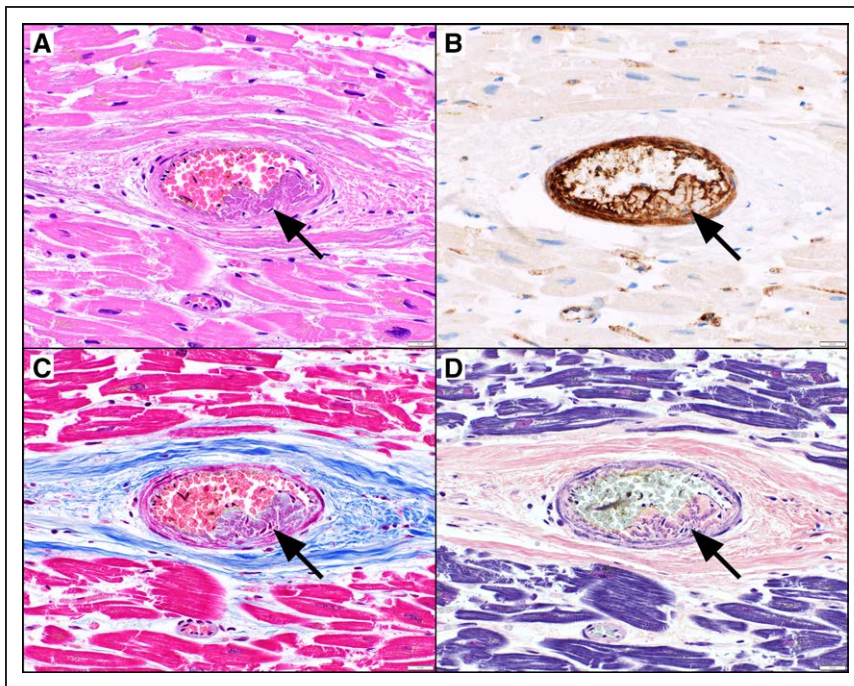


Figure 2. Ancillary testing of fibrin microthrombi.

The presence of fibrin within the small vascular thrombi (A, hematoxylin and eosin) was confirmed with Factor VIII immunohistochemistry (B), Masson trichrome stain, which stains fibrin red (C), and phosphotungstic acid hematoxylin, which stains fibrin dark blue (D) (arrows; all, 400× original magnification).

Patients with cardiac amyloidosis showed intense sarcolemmal staining, in comparison with those without (Figure 7).

Of the COVID-19 cohort, 40% had a history of angiotensin converting enzyme (ACE)-inhibitor use, compared with 33% of the influenza cases and 0% of the

control cases. Pharmacological upregulation of ACE2 mRNA has been documented in animal studies in response to ACE-inhibitor administration.¹⁴ Thus, this interesting trend is opposite of what would be expected because of the pharmacological heterogeneity among our study groups.

Table 3. Summary of Cardiac Pathology

Characteristics	COVID-19* (n=15)	Active COVID-19† (n=12)	Influenza (n=6)	Controls (n=6)	P value‡	Pairwise comparison for significant values
Gross characteristics						
Heart weight, g, median (range)	443.1 (286.3–545.0)	474.0 (286.3–545.0)	398.4 (269.0–592.0)	244.5 (197.0–560.3)	0.22§	
Expected heart weight,¶ %, median (range)	1.42 (0.97–1.94)	1.49 (0.97–1.94)	1.35 (1.04–2.13)	0.89 (0.78–2.11)	0.17§	
Histopathologic characteristics						
Microthrombosis, n (%)	12 (80.0)	11 (91.7)	2 (33.3)	2 (33.3)	0.006¶	COVID-19 vs influenza, <i>P</i> =0.02 COVID-19 vs control, <i>P</i> =0.02
Involved arterioles, median % of total (range)	6.3 (0.0–28.6)	7.3 (0.0–28.6)	0.0 (0.0–6.1)	0.0 (0.0–4.7)	0.003§	COVID-19 vs influenza, <i>P</i> =0.01 COVID-19 vs control, <i>P</i> =0.003
Myocarditis, n (%)	5 (33.3)	4 (33.3)	1 (16.7)	0 (0.0)	0.38¶	
Interstitial edema, n (%)	0 (0.0)	0 (0.0)	2 (33.3)	0 (0.0)	0.11¶	
Acute ischemic injury, n (%)	2 (13.3)	2 (16.7)	2 (33.3)	0 (0.0)	0.32¶	

COVID-19 indicates coronavirus disease 2019.

*Including both patients with active and cleared severe acute respiratory syndrome coronavirus 2 viral infection.

†COVID-19 cases with cleared infection excluded (n=3).

‡Denotes overall *P* value including active COVID-19, influenza, and control cases.

§Kruskal-Wallis test.

¶Compared with age-, sex-, and weight-based controls.¹³

¶Fisher exact test.

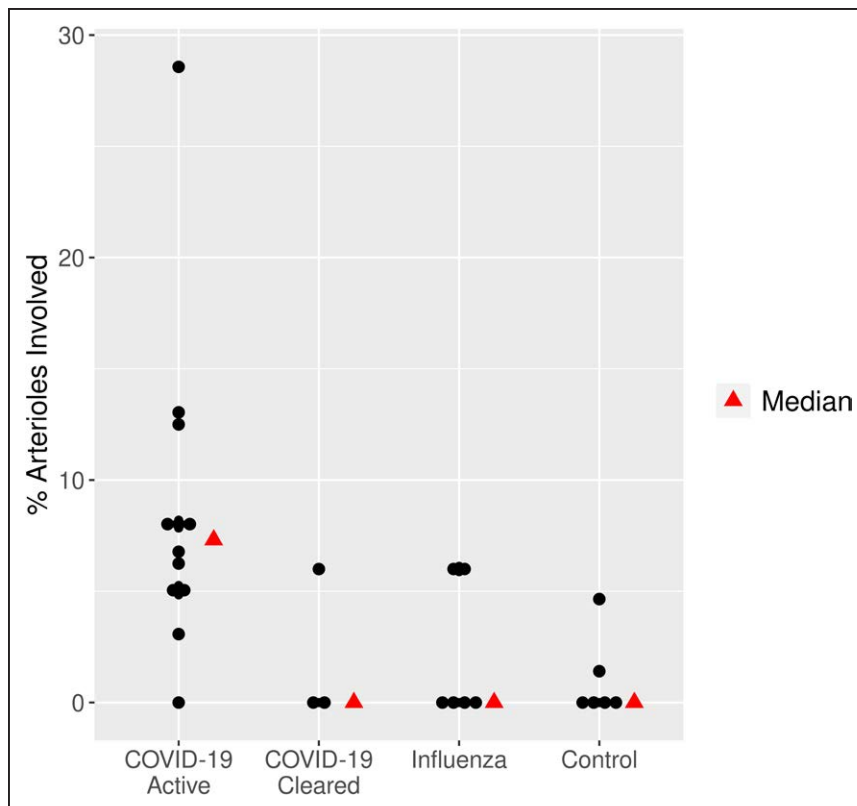


Figure 3. Frequency of fibrin microthrombi. Active coronavirus disease 2019 (COVID-19) cases showed more frequent fibrin microthrombi than other postmortem control groups, including both virally mediated (Influenza) and nonvirally mediated (Control) deaths.

SARS-CoV-2 Immunohistochemistry

Immunohistochemical evaluation for SARS-CoV-2 nucleocapsid antibodies showed focal, nonspecific staining in all cases tested (n=4, all active disease, patients A1 to A3, A5). Nonspecific staining included 3 patients with weak endothelial cell staining (arteriolar and capillary), whereas endocardial staining and intramural macrophage staining was observed in 1 patient each.

Droplet Digital Polymerase Chain Reaction

Viral nucleic acid amplification through ddPCR was negative in cardiac tissue from patients with COVID-19 (mean number of acceptable droplets analyzed per case, 11932). Nine cases had matched lung specimens evaluated by ddPCR (8 with active COVID-19; 1 cleared). All active lung specimens tested positive for SARS-CoV-2 by ddPCR; the 1 cleared case was negative (Figure 8; Table III in the Data Supplement).

DISCUSSION

The novel β -coronavirus SARS-CoV-2 and the resulting global pandemic has not only drastically changed our social framework, but has made an indelible impact on the medical and scientific community. Although great strides have been made in characterizing the virus and its clinical effects, much remains unknown about COVID-19 and the

intricacies of its pathological mechanisms. Detailed, organ-specific, pathological evaluation of both infected patients and patients with resolved infections can provide potentially actionable insight into the pathogenicity of SARS-CoV-2. This study presents a detailed examination of the myocardial histopathology in patients with COVID-19 and is the first to describe findings in patients who have cleared the virus. SARS-CoV-2 molecular and immunohistochemical evaluation of the myocardium was performed.

It is now well established that SARS-CoV-2 infects host cells through the ACE2-receptor and that this receptor's relative abundance in pulmonary epithelium likely facilitates infection.¹⁵ Consequently, the relationship of SARS-CoV-2 with endothelial cells and ACE2 receptors has been explored in the literature. Of particular interest is the suggestion that viral infection may induce inflammatory changes, damaging endothelium with resultant thrombosis.¹⁶ Theories of a virally mediated acquired coagulopathy have been bolstered by documentation of the virus in endothelial cells¹⁶ and reports suggesting that SARS-CoV-2 infection may be complicated by thrombotic or thromboembolic presentations.^{17,18} Adding credence to this theory are reports of vascular thrombi on postmortem examination.¹⁹

Nonocclusive Fibrin Microthrombi: The Role of Direct Viral Invasion

Fibrin microthrombi/microthromboemboli have been documented in case reports and small series of

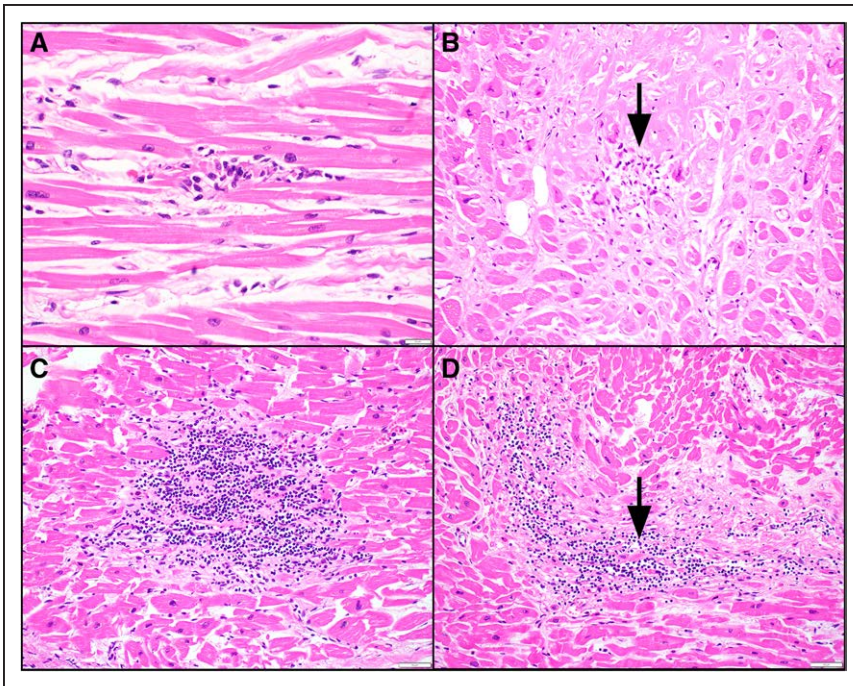


Figure 4. Myocarditis in COVID-19. Active myocarditis was identified in 5 COVID-19 cases. Four such cases occurred in the setting of active COVID-19 infection and were generally limited in extent, including focal active lymphocytic myocarditis (A, 400× original magnification) and focal active lymphohistiocytic myocarditis associated with amyloid deposition (B, arrow, 400× original magnification). One cleared COVID-19 case showed extensive, multifocal, smoldering myocarditis in a background of fibrosis, suggesting chronicity to the process (C, 200× original magnification), with residual active disease (D, arrow, 200× original magnification; hematoxylin and eosin stain). COVID-19 indicates coronavirus disease 2019.

postmortem examinations, particularly affecting the pulmonary vasculature.^{7,12,19–21} This also appears to be the case in the heart, with fibrin microthrombi being found in most COVID-19 cases in this series

and to a greater extent than either virally mediated deaths or controls.

The mechanism of fibrin microthrombosis in the heart is unclear. The literature acknowledges a

Patient	Non-occlusive fibrin microthrombi*	Mural thrombi	Myocarditis	Interstitial edema	Acute ischemic changes	Amyloid	
<i>Active COVID-19</i>							
A1	Diffuse	Absent	Absent	Absent	Absent	Absent	
A2	Diffuse	Absent	Absent	Absent	Absent	Occasional	
A3	Diffuse	Absent	Absent	Absent	Absent	Absent	
A4	Diffuse	Absent	Absent	Absent	Absent	Absent	
A5	Diffuse	Absent	Absent	Absent	Absent	Absent	
A6	Diffuse	Absent	Absent	Absent	Absent	Absent	
A7	Diffuse	Absent	Absent	Absent	Absent	Absent	
A8	Absent	Absent	Diffuse	Absent	Absent	Absent	
A9	Absent	Absent	Absent	Absent	Absent	Absent	
A10	Diffuse	Absent	Absent	Absent	Absent	Absent	
A11	Absent	Absent	Absent	Absent	Absent	Absent	Absent
A12	Diffuse	Absent	Absent	Absent	Absent	Absent	Rare/Isolated
<i>Cleared COVID-19</i>							
C1	Diffuse	Absent	Absent	Absent	Absent	Occasional	
C2	Absent	Absent	Absent	Absent	Absent	Absent	
C3	Absent	Absent	Diffuse	Absent	Absent	Absent	Diffuse

Figure 5. Semiquantitative summary of histological findings in patients with COVID-19. Nonocclusive fibrin thrombi were the most common finding in patients who died of or after of severe acute respiratory syndrome coronavirus 2 infection (*Rare/isolated: <5%; Occasional: ≥5% and <10%; and Diffuse: ≥10%). Additional pertinent findings included myocarditis and underlying cardiac amyloidosis. COVID-19 indicates coronavirus disease 2019.

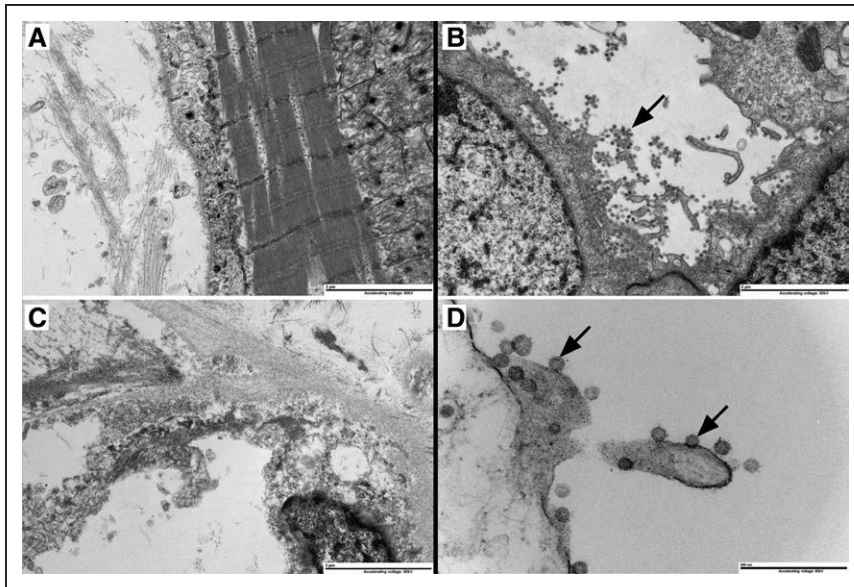


Figure 6. Ultrastructural analysis.

No viral particles were identified within the cardiac myocytes (A) or endothelial cells (C) of the COVID-19 cases. Numerous viral particles were identified on a positive control slide produce from virally infected Vero cell lines (arrows, B and D). COVID-19 indicates coronavirus disease 2019.

SARS-CoV-2–mediated systemic acquired coagulopathy, distinct from disseminated intravascular coagulation and thrombotic microangiopathy.²² This hypercoagulable state may be attributable, at least in part, to direct invasion of endothelial cells, with cellular membrane disruption and subsequent endothelial injury. This theory is based on ultrastructurally identified intracellular virus.¹⁹ Despite these compelling findings in lung tissue, we were unable to document conclusive viral presence in the heart (endothelial cells or myocytes) through immunohistochemical or ultrastructural means. Furthermore, ddPCR studies were negative for viral nucleic acid.

This is particularly perplexing in light of previous experience with myocardial involvement by severe acute

respiratory syndrome coronavirus (SARS-CoV), the virus responsible for the 2003 outbreak. A contemporaneous study by Oudit and colleagues²² showed that the SARS-CoV genome was detectable by real-time PCR in the myocardium of 35% of patients who died of the disease. This stands in contrast with SARS-CoV-2 in our study. The same study also showed downregulation of ACE2 receptors in myocardium infected by SARS-CoV, a finding mirrored in patients with SARS-CoV-2.²⁴ We were unable to demonstrate a qualitative difference in myocardial ACE2 staining through immunohistochemical means between patients with COVID-19 and either control cohorts.

There was, however, significantly decreased arteriolar endothelial expression of ACE2 receptors in patients

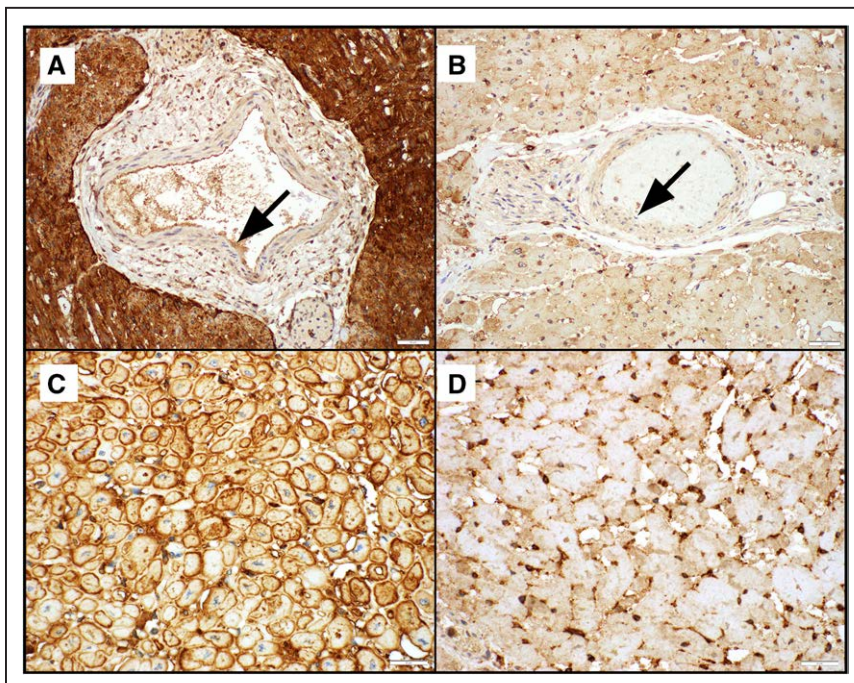


Figure 7. Angiotensin-converting enzyme 2 receptor immunohistochemistry.

Endothelial cell staining in small arteries and arterioles showed significantly greater staining in controls (A), in comparison with patients who had COVID-19 (B) (arrows, 400× original magnification). Sarcolemmal staining was observed to be accentuated in cases of cardiac amyloidosis (C), in comparison with patients without cardiac amyloid (D) (600× original magnification). COVID-19 indicates coronavirus disease 2019.

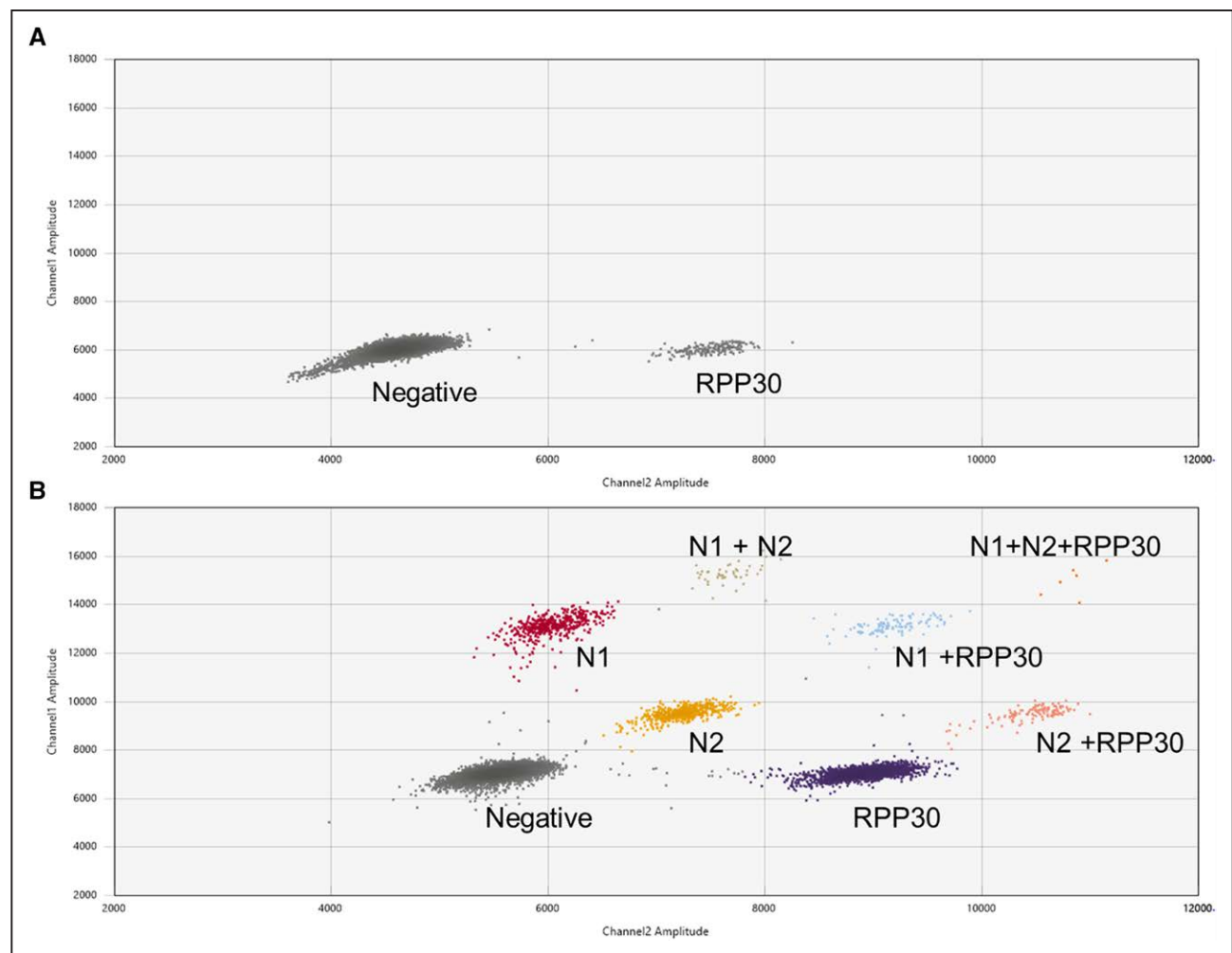


Figure 8. Droplet digital polymerase chain reaction results.

A, Negative myocardial sample showing droplets in the control gene without droplets in viral genome regions (N1 or N2 [nucleocapsid 1 or 2]). **B**, Positive lung sample showing multiple droplets in viral N1 and N2 regions and droplets in control gene (RPP30), as well. Note: Because of the high number of severe acute respiratory syndrome coronavirus 2 genome copies in the sample, some droplets harbor 2 nucleic acid sequences (control and N1/N2 sequences) in the same droplet, causing signals in unique labeled regions (eg, N1+N2, N1+RPP30).

with COVID-19 on blinded review. This finding indirectly suggests possible virally mediated ACE2 suppression and attractively offers a potential explanation of the observed in situ microthrombosis. However, as mentioned, we were not able to substantiate this by the direct demonstration of virus by either antigenic or molecular genetic means. It is possible that either the virus has cleared from endothelial cells or, alternatively, that a separate mechanism may be responsible for microthrombosis.

Nonocclusive Fibrin Microthrombi: The Role of Systemic Coagulopathy

The transmembrane enzyme ACE2 catalyzes the conversion of angiotensin II to angiotensin in vivo. Virally mediated downregulation of ACE2 receptors subsequently interferes with the receptor's physiological responsibilities. Angiotensin, among its other properties, promotes antithrombotic homeostasis through binding

to the Mas receptor on the platelet membrane. Mas receptor knockout animal models exhibit decreased bleeding time and increased thrombosis, which is corrected by administration of angiotensin.^{25,26} Based on these data, ACE2 receptor downregulation may promote a prothrombotic state through decreased circulating levels of angiotensin.²⁴

Potentiating this effect is the likely contribution of immune (over)activation. COVID-19 has been described in 3 (sometimes overlapping) phases of disease: initial infection, pulmonary phase, and hyperinflammation.²⁷ During hyperinflammation, a cellular immune response to viral invasion elaborates cytokines and inflammatory markers mediating further inflammation and cellular/endothelial permeability. Patients with severe disease have been shown to have high levels of IL-6 (interleukin-6), IL-2, IL-7, and tumor necrosis factor- α .^{3,28} This results in homeostatic imbalance, favoring fibrin formation over fibrinolysis.

Myocarditis and Acute Ischemic Injury

Elevated troponins have been documented in COVID-19 cases and portend a worse outcome. Several mechanisms for this finding have been proposed, including myocardial injury from circulating cytokines, myocarditis, and ischemia (the latter including microangiopathic occlusion, epicardial coronary artery plaque rupture from virally induced instability, and supply/demand mismatch).²⁹ In our limited series, focal active lymphocytic myocarditis was observed in one-third of cases; however, the majority were very limited despite extensive myocardial sampling. This calls into question the notion that myocarditis contributes significantly to myocardial injury in many patients with COVID-19. Notwithstanding, fulminant myocarditis certainly does appear to be a manifestation of COVID-19, albeit not a common one.³⁰ Acute ischemic changes were also observed in only 2 COVID-19 cases. These findings add credence to the possibility of myocardial injury from circulating cytotoxins (eg, cytokines), or troponin leak secondary to myocardial strain.

Amyloidosis

Our series contained a high proportion of individuals with cardiac amyloidosis (26.7%); to a degree, that far exceeds the autopsy prevalence of cardiac amyloidosis at our institution, which has been 3.7% over the past 2 years. A similar incidence rate was recently reported as an ancillary finding in a cases series of 21 COVID-19 autopsies with 29% of decedents showing immunohistochemical evidence of transthyretin amyloidosis in the myocardium and 14% of patients showing amyloid deposition in the pulmonary vasculature.³⁰ This suggests a specific group of patients that may be at high risk of morbidity and mortality from SARS-CoV-2 infection.

A single case of amyloidosis had concomitant myocardial inflammation. There is a known association of myocardial inflammation in the setting of amyloidosis, potentially confounding the finding in this patient for the purposes of this study.

Long-Term Sequelae: Persistent Pathology After Clearance of SARS-CoV-2

Less than 1 year into this pandemic, it is not only our understanding of the pathobiology of COVID-19 that is incomplete, but also our appreciation for the long-term effects of the disease. Chronic complications involving the lung and heart have begun to emerge.^{31,32} Clinical and radiological data are supported by early pathology data in the lungs of those with cleared infection.³³ Our series now adds to the literature histopathologic cardiac findings from 3 patients with such cleared infection. Although the number is too small to draw definitive

conclusions, these cases likely represent (at least) 3 possible outcomes after viral clearance. One patient died of unrelated causes, following positive antibody testing in the absence of profound clinical symptomatology. A second patient had continued demonstration of microthrombosis despite viral clearance, suggesting that the cardiovascular consequences extend beyond the active infectious stage. Last, following negative viral PCR, a third patient was placed on extracorporeal membrane oxygenation with significant bleeding complications and no myocardial thrombi. This patient also showed ongoing, smoldering active lymphocytic myocarditis in a background of fibrosis, suggesting chronicity to the condition, and (similar to the aforementioned patient) likely contributed to adverse cardiovascular complications beyond the duration of active viral infection.

Limitations

This series and the observations herein are based on a limited number of patients and controls, thus good representation across the sex and ethnicity spectrum was not achieved. Furthermore, the variability in clinical presentation and course was accompanied by heterogeneous treatment regimens, which may certainly impact the spectrum of findings described. Uniformity in testing and workup was not observed due to the inherent retrospective clinical component of the study design. Internal referral bias of our patient population is also limiting. Cross-sectional cardiac imaging was not performed in any of the study patients during their illness.

CONCLUSIONS

This series is dedicated exclusively to the cardiac histopathologic, immunohistochemical, ultrastructural, and molecular findings in patients who died of active or cleared SARS-CoV-2 infection. Although the preceding data have documented the virus in endothelial cells, no definitive evidence of myocardial infection was present in this series. Our data show that COVID-19 cases frequently have fibrin cardiac microthrombi in the absence of acute ischemic injury, potentially explaining why some have observed reduced COVID-19–associated mortality in the setting of systemic anticoagulation.³⁴ Moreover, myocarditis is present in one-third of patients with COVID-19, but limited in extent and not likely to explain the totality of cardiac symptoms or findings in this population.

Histological features of cleared infection do not appear to differ significantly from active disease, although the proximity of infection to death likely heavily influences this finding. We also suggest cardiac amyloidosis as an additional possible risk factor for severe disease based on its frequency in this study.

ARTICLE INFORMATION

Received August 7, 2020; accepted November 12, 2020.

Continuing medical education (CME) credit is available for this article. Go to <http://cme.ahajournals.org> to take the quiz.

The Data Supplement is available with this article at <https://www.ahajournals.org/doi/suppl/10.1161/CIRCULATIONAHA.120.050754>.

Correspondence

Joseph J. Maleszewski, MD, Mayo Clinic, 200 First Street SW, Rochester, MN 55905. Email maleszewski.joseph@mayo.edu

Affiliations

Department of Laboratory Medicine and Pathology (M.C.B., N.A.B., A.J.L., M.-C.A., M.P.A., A.C.R., C.E.H., R.A.Q., R.M., B.R.K., P.T.L., J.J.M.), Division of Biomedical Statistics and Informatics (S.M.J.), Department of Cardiovascular Medicine (J.J.M.), Mayo Clinic, Rochester, MN. Arkana Laboratories, Little Rock (C.L.). Division of Vascular Surgery, Mayo Clinic, Jacksonville, FL (Y.E.).

Acknowledgments

The authors extend gratitude to A. Bridgeman for her technical expertise in obtaining the molecular data and Mr Jon Charlesworth and the electron microscopy laboratory at Mayo Clinic for their technical skills and expertise. Furthermore, the authors acknowledge K. Tindal, E. Markell, and T. Siebenaler for their contributions of time and administration related to tissue processing. The authors also acknowledge Drs. Norgan, Righi, Horton, Villalobos and Ebner, P. Hurst, and pathologists' assistants E. H. Cheek, N. Steinle, P. Brown, and R. Larsen for their astute case management of the reported patients.

Sources of Funding

None.

Disclosures

None.

Supplemental Materials

Data Supplement Tables I–III

REFERENCES

- Atri D, Siddiqi HK, Lang JP, Nauffal V, Morrow DA, Bohula EA. COVID-19 for the cardiologist: basic virology, epidemiology, cardiac manifestations, and potential therapeutic strategies. *JACC Basic Transl Sci*. 2020;5:518–536. doi: 10.1016/j.jacbs.2020.04.002
- Bos JM, Hebl VB, Oberg AL, Sun Z, Herman DS, Teekakirikul P, Seidman JG, Seidman CE, Dos Remedios CG, Maleszewski JJ, et al. Marked up-regulation of ACE2 in hearts of patients with obstructive hypertrophic cardiomyopathy: implications for SARS-CoV-2-mediated COVID-19. *Mayo Clin Proc*. 2020;95:1354–1368. doi: 10.1016/j.mayocp.2020.04.028
- Zhou F, Yu T, Du R, Fan G, Liu Y, Liu Z, Xiang J, Wang Y, Song B, Gu X, et al. Clinical course and risk factors for mortality of adult inpatients with COVID-19 in Wuhan, China: a retrospective cohort study [published correction appears in *Lancet*. 2020;395:1038]. *Lancet*. 2020;395:1054–1062. doi: 10.1016/S0140-6736(20)30566-3
- Arentz M, Kim E, Klaff L, Lokhandwala S, Riedo FX, Chong M, Lee M. Characteristics and outcomes of 21 critically ill patients with COVID-19 in Washington State. *JAMA*. 2020;323:1612–1614. doi: 10.1001/jama.2020.4326
- Guo T, Fan Y, Chen M, Wu X, Zhang L, He T, Wang H, Wan J, Wang X, Lu Z. Cardiovascular implications of fatal outcomes of patients with coronavirus disease 2019 (COVID-19). *JAMA Cardiol*. 2020;5:811–818. doi: 10.1001/jamacardio.2020.1017
- Yan L, Mir M, Sanchez P, Beg M, Peters J, Enriquez O, Gilbert A. COVID-19 in a Hispanic woman. *Arch Pathol Lab Med*. 2020;144:1041–1047. doi: 10.5858/arpa.2020-0217-SA
- Buja LM, Wolf DA, Zhao B, Akkanti B, McDonald M, Lelenwa L, Reilly N, Ottaviani G, Elghetany MT, Trujillo DO, et al. The emerging spectrum of cardiopulmonary pathology of the coronavirus disease 2019 (COVID-19): report of 3 autopsies from Houston, Texas, and review of autopsy findings from other United States cities. *Cardiovasc Pathol*. 2020;48:107233. doi: 10.1016/j.carpath.2020.107233
- Barton LM, Duval EJ, Stroberg E, Ghosh S, Mukhopadhyay S. COVID-19 autopsies, Oklahoma, USA. *Am J Clin Pathol*. 2020;153:725–733. doi: 10.1093/ajcp/aaqa062
- Schaller T, Hirschi K, Burkhardt K, Braun G, Trepel M, Märkl B, Claus R. Postmortem examination of patients with COVID-19. *JAMA*. 2020;323:2518–2520. doi: 10.1001/jama.2020.8907
- Fox SE, Akmatbekov A, Harbert JL, Li G, Quincy Brown J, Vander Heide RS. Pulmonary and cardiac pathology in African American patients with COVID-19: an autopsy series from New Orleans. *Lancet Respir Med*. 2020;8:681–686. doi: 10.1016/S2213-2600(20)30243-5
- Rapkiewicz AV, Mai X, Carsons SE, Pittaluga S, Kleiner DE, Berger JS, Thomas S, Adler NM, Charytan DM, Gasmi B, et al. Megakaryocytes and platelet-fibrin thrombi characterize multi-organ thrombosis at autopsy in COVID-19: a case series. *EClinicalMedicine*. 2020;24:100434. doi: 10.1016/j.eclinm.2020.100434
- Basso C, Leone O, Rizzo S, De Gaspari M, van der Wal AC, Aubry MC, Bois MC, Lin PT, Maleszewski JJ, Stone JR. Pathological features of COVID-19-associated myocardial injury: a multicentre cardiovascular pathology study. *Eur Heart J*. 2020;41:3827–3835. doi: 10.1093/eurheartj/ehaa664
- Kitzman DW, Scholz DG, Hagen PT, Ilstrup DM, Edwards WD. Age-related changes in normal human hearts during the first 10 decades of life. Part II (maturity): a quantitative anatomic study of 765 specimens from subjects 20 to 99 years old. *Mayo Clin Proc*. 1988;63:137–146. doi: 10.1016/S0025-6196(12)64946-5
- Ferrario CM, Jessup J, Chappell MC, Averill DB, Brosnihan KB, Tallant EA, Diz DI, Gallagher PE. Effect of angiotensin-converting enzyme inhibition and angiotensin II receptor blockers on cardiac angiotensin-converting enzyme 2. *Circulation*. 2005;111:2605–2610. doi: 10.1161/CIRCULATIONAHA.104.510461
- Yuki K, Fujioji M, Koutsogiannaki S. COVID-19 pathophysiology: a review. *Clin Immunol*. 2020;215:108427. doi: 10.1016/j.clim.2020.108427
- Varga Z, Flammer AJ, Steiger P, Haberecker M, Andermatt R, Zinkernagel AS, Mehra MR, Schuepbach RA, Ruschitzka F, Moch H. Endothelial cell infection and endotheliitis in COVID-19. *Lancet*. 2020;395:1417–1418. doi: 10.1016/S0140-6736(20)30937-5
- Avula A, Nalleballe K, Narula N, Sapozhnikov S, Dandu V, Toom S, Glaser A, Elsayegh D. COVID-19 presenting as stroke. *Brain Behav Immun*. 2020;87:115–119. doi: 10.1016/j.bbi.2020.04.077
- Bikdeli B, Madhavan MV, Jimenez D, Chuich T, Dreyfus I, Driggin E, Nigoghossian C, Ageno W, Madjid M, Guo Y, et al; Global COVID-19 Thrombosis Collaborative Group, Endorsed by the ISTH, NATF, ESVM, and the IUA, Supported by the ESC Working Group on Pulmonary Circulation and Right Ventricular Function. COVID-19 and thrombotic or thromboembolic disease: implications for prevention, antithrombotic therapy, and follow-up: JACC state-of-the-art review. *J Am Coll Cardiol*. 2020;75:2950–2973. doi: 10.1016/j.jacc.2020.04.031
- Ackermann M, Verleden SE, Kuehnel M, Haverich A, Welte T, Laenger F, Vanstapel A, Werlein C, Stark H, Tzankov A, et al. Pulmonary vascular endothelialitis, thrombosis, and angiogenesis in Covid-19. *N Engl J Med*. 2020;383:120–128. doi: 10.1056/NEJMoa2015432
- Wichmann D, Sperhake JP, Lütgehetmann M, Steurer S, Edler C, Heinemann A, Heinrich F, Mushumba H, Kniep I, Schröder AS, et al. Autopsy findings and venous thromboembolism in patients with COVID-19: a prospective cohort study. *Ann Intern Med*. 2020;173:268–277. doi: 10.7326/M20-2003
- Roden AC, Bois MC, Johnson TF, Aubry MC, Alexander MP, Hagen CE, Lin PT, Quinton RA, Maleszewski JJ, Boland JM. The spectrum of histopathologic findings in lungs of patients with fatal COVID-19 infection [published online August 21, 2020]. *Arch Pathol Lab Med*. doi: 10.5858/arpa.2020-0491-SA <https://meridian.allenpress.com/aplm/article-lookup/doi/10.5858/arpa.2020-0491-SA>
- Iba T, Levy JH, Levi M, Connors JM, Thachil J. Coagulopathy of coronavirus disease 2019. *Crit Care Med*. 2020;48:1358–1364. doi: 10.1097/CCM.0000000000004458
- Oudit GY, Kassiri Z, Jiang C, Liu PP, Poutanen SM, Penninger JM, Butany J. SARS-coronavirus modulation of myocardial ACE2 expression and inflammation in patients with SARS. *Eur J Clin Invest*. 2009;39:618–625. doi: 10.1111/j.1365-2362.2009.02153.x
- Verdecchia P, Cavallini C, Spanevello A, Angeli F. The pivotal link between ACE2 deficiency and SARS-CoV-2 infection. *Eur J Intern Med*. 2020;76:14–20. doi: 10.1016/j.ejim.2020.04.037

25. Fraga-Silva RA, Pinheiro SV, Gonçalves AC, Alenina N, Bader M, Santos RA. The antithrombotic effect of angiotensin-(1-7) involves mas-mediated NO release from platelets. *Mol Med*. 2008;14:28–35. doi: 10.2119/2007-00073.Fraga-Silva
26. Fraga-Silva RA, Costa-Fraga FP, De Sousa FB, Alenina N, Bader M, Sinisterra RD, Santos RA. An orally active formulation of angiotensin-(1-7) produces an antithrombotic effect. *Clinics (Sao Paulo)*. 2011;66:837–841. doi: 10.1590/s1807-59322011000500021
27. Akhmerov A, Marbán E. COVID-19 and the heart. *Circ Res*. 2020;126:1443–1455. doi: 10.1161/CIRCRESAHA.120.317055
28. Ruan Q, Yang K, Wang W, Jiang L, Song J. Clinical predictors of mortality due to COVID-19 based on an analysis of data of 150 patients from Wuhan, China. *Intensive Care Med*. 2020;46:846–848. doi: 10.1007/s00134-020-05991-x
29. Tersalvi G, Vicenzi M, Calabretta D, Biasco L, Pedrazzini G, Winterton D. Elevated troponin in patients with coronavirus disease 2019: possible mechanisms. *J Card Fail*. 2020;26:470–475. doi: 10.1016/j.cardfail.2020.04.009
30. Menter T, Haslbauer JD, Nienhold R, Savic S, Hopfer H, Deigendesch N, Frank S, Turek D, Willi N, Pargger H, et al. Postmortem examination of COVID-19 patients reveals diffuse alveolar damage with severe capillary congestion and variegated findings in lungs and other organs suggesting vascular dysfunction. *Histopathology*. 2020;77:198–209. doi: 10.1111/his.14134
31. Puntmann VO, Carerj ML, Wieters I, Fahim M, Arendt C, Hoffmann J, Shchendrygina A, Escher F, Vasa-Nicotera M, Zeiher AM, et al. Outcomes of cardiovascular magnetic resonance imaging in patients recently recovered from coronavirus disease 2019 (COVID-19). *JAMA Cardiol*. 2020;e203557.
32. Chen JY, Qiao K, Liu F, Wu B, Xu X, Jiao GQ, Lu RG, Li HX, Zhao J, Huang J, et al. Lung transplantation as therapeutic option in acute respiratory distress syndrome for coronavirus disease 2019-related pulmonary fibrosis. *Chin Med J (Engl)*. 2020;133:1390–1396. doi: 10.1097/CM9.0000000000000839
33. Polak SB, Van Gool IC, Cohen D, von der Thüsen JH, van Paassen J. A systematic review of pathological findings in COVID-19: a pathophysiological timeline and possible mechanisms of disease progression. *Mod Pathol*. 2020;33:2128–2138. doi: 10.1038/s41379-020-0603-3
34. Kamel A, Sobhy M, Magdy N, Sabry N, Farid S. Anticoagulation outcomes in hospitalized Covid-19 patients: a systematic review and meta-analysis of case-control and cohort studies. *Rev Med Virol*. 2020;6:e2180. doi: 10.1002/rmv.2180